[1.]Sarbojit MUKHERJEE

A SEPIC-CUK-CSCCC BASED SIMO CONVERTER DESIGN USING PSO-MPPT FOR RENEWABLE ENERGY APPLICATION

[1.] Electrical Engineering Department, RCC Institute of Information Technology, Kolkata, West-Bengal, INDIA

Abstract: This paper presents the operation of Single Input Multiple Output (SIMO) converter using the SEPIC-Cuk-Canonical Switching Cell Combination Converter (SEPIC-Cuk-CSCCC) topology, supplied from a Solar Photo Voltaic (SPV) source. As the output of the SPV depends on the ambient condition like solar radiation and temperature, a Particle Swarm Optimization (PSO) based Maximum Power Point Tracking (MPPT) method is applied to maintain the SPV operating point at Maximum Operating Point (MPP) always. This SIMO converter produces three different output voltage (both positive and negative polarity). Reduced converter size and the cost with higher efficiency can be achieved in this topology as only one controllable switch along with less number of components is used. A simulation has been carried out to verify the operation of the PSO-MPPT based SIMO converter. Simulation results show satisfactory MPPT operation. Besides, it is also shown that for SIMO applications, a combination of Single Input Single Output (SISO) converter is preferable.
Keywords: PSO-MPPT, SPV application, SIMO converter, DC-DC converter

INTRODUCTION

To meet the growing power demand without any environmental issues, renewable energy sources are the most eligible option in the recent era. Continuous decrement of the cost of the Solar Photo Voltaic (SPV) makes itself more valuable for future research and implementation [1]. Besides that, the SPV system has the advantages of the absence of rotating parts, minimum maintenance, and almost zero environmental loss [2], [3].

The power characteristics of the renewable energy source are nonlinear in nature because of the dependency on solar irradiance, ambient temperature. There exists one operating point where they generate maximum power which is observed in the solar P-V and the V-I characteristics. In order to take full advantage of available energy resource and achieve maximum utilization efficiency, maximum power point tracking (MPPT) control techniques which extracts maximum power from the renewable source is essential. Several researchers prescribed different MPPT methods for extracting maximum power[4]. Based on the involvement of several control variables, types of control strategies, nature of the available circuitry, and cost of applications are the main factors to select the MPPT algorithm.

The evolution of developing DC-DC converter has been constant over the past year. The requirement of different voltage and power level across the power electronics devices in different applications enhances the growth of the development of the DC-DC converter. So not only the single quadrant converter, multi-level and multi quadrant converter has become famous day by day for its new control strategy and topologies, which cause the efficiency improvement and the reduction of size.

There are a variety of applications where multiple dc outputs with different voltage levels are required from a single power supply as step-up, step-down, and sometimes both step-up/down mode.

For such application, a multi-port DC-DC converter provides the best solution. Single input multiple output (SIMO) converter is one of the well-known multi-port converter used for such application. i.e. Hybrid/ Electric Vehicles (EHV), microelectronics, telecommunication, lighting, etc. Increased efficiency with reduced cost can be achieved in the SIMO converter as less number component is used.

In this paper, a SEPIC Cuk CSC combination converter-based SIMO converter, connected with a SPV is proposed where a single switch is shared by all of these converters which provides simplification in control. A Particle Swarm Optimization (PSO) based MPPT control is implemented to extract maximum power from the SPV. In the proposed converter SEPIC converter provide positive voltage output. Besides this Cuk and CSC converter produced a negative output voltage. A simulation model is developed in MATLAB/Simulink software and the verification of PSO – MPPT based SIMO converter output is verified.

This article mainly focuses on the operation and design PSO-MPPT based SEPIC Cuk CSC converter. The complete structure of the proposed topology is described in section 2. The PSO based MPPT algorithm along with the converter working are discussed in section 3. Section 4 describes the control analysis of the proposed topology.Simulation results are shown in section 5.

PROPOSED TOPOLOGY

In [5]–[7], basic topologies of the non-isolated converter is introduced for solar PV application. Besides the conventional topologies, a combination of these converters can sometimes found advantageous in many applications as given in [8]–[10]. A comparative study of different MPPT techniques for a basic converter with their performance analysis is also described in [4]. PSO based MPPT algorithm is preferred over conventional technique like perturb and observe (P and O) and incremental conductance (IC).

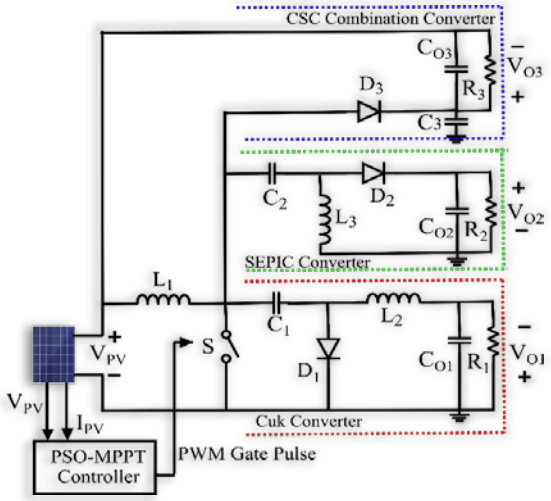

Figure 1. Proposed SEPIC-Cuk-CSC Converter

In this paper, a SEPIC-Cuk-CSC combinational SIMO converter is proposed (fig 1) where a PSO based MPPT technique is applied to extract maximum solar PV power.

OPERATING PRINCIPAL

— PSO – MPPT Algorithm

Particle Swarm Optimization (PSO) is a population-based intelligence optimization technique, inspired by the foraging behavior of a flock of birds and fish schooling in search of food. In PSO algorithm individual birds are referred to as an individual flying particle that has its own fitness value. Each particle movement, in terms of direction and distance, as calculated by the objective function and the velocity of the individual particle. Exchange of information between the particles happened based on their search process. P_{best} and G_{best} are the best position of the individual particle and the best position of the all the particle, comparing all the P_{best} , respectively. All the swarm updates their direction and velocity to move towards the best position. So, the convergence can be achieved[11]–[13]. The standard PSO algorithm can be represented by

$$v_i(k+1)=wv_i(k)+c_1r_1\left(P_{best}-x_i(k)\right)+c_2r_2\left(G_{best}-x_i(k)\right) \quad (1)$$

$$P_{best}=x_{ik} \quad (2)$$

$$f\left(x_{ik}\right)>f\left(P_{best,i}\right) \quad (3)$$

$$x_i(k+1)=x_i(k)+v_i(k+1) \quad (4)$$

where $i=1,2.....N$. v_i and x_i are the velocity and the position of the particle i , the number of iteration denoted by k, w represents the inertia weight. r_1 and r_2 are the uniformly distributed random variable within [0 and 1]. Cognitive and social coefficients are denoted by c_1 and c_2 . P_{best} and G_{best} represent the individual best position of i^{th} particle and the swarm best position of all the particle. If equation 5 is satisfied then the value of the P_{best} can be updated by equation 6.

$$f\left(x_{ik}\right)>f\left(P_{best,i}\right) \quad (5)$$

$$P_{best}=x_{ik} \quad (6)$$

where, f represents the objective function that should be maximized.

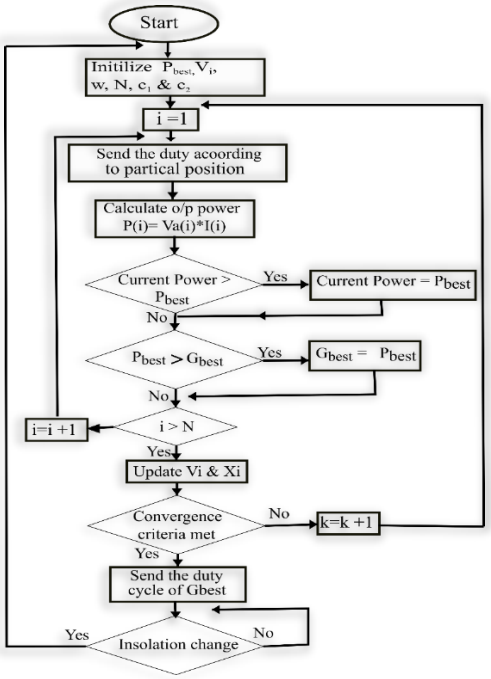

Figure 2. PSO based MPPT algorithm flowchart.

In Figure 2, the PSO based MPPT topology is described. As given in the flowchart at the beginning particle swarm position and fitness value evaluation function are defined as the duty cycle and the generated output power respectively. A random initialization, within a uniform distribution, is made for the position and the velocity of each particle. After that the fitness value of the particle is calculated, it is updated comparing with the previous value. P_{best} and G_{best} of each particle are also update against the previous values. Thereafter particle velocities and positions are updated accordingly.

With the new value of v_i and x_i , the convergence criteria are checked, which are either optimal solution localization or reaching the maximum number of iteration. Depending upon the weather condition and the load value, the fitness function becomes variable. So, the PSO must be reinitialized to search a new MPP as the output of the PV module changed.

— Single Input Multiple Output(SIMO Converter)

In this section, an interesting combination of SEPIC Cuk CSC combination converter topology is introduced. The ability to produce both positive and negative voltage simultaneously makes this converter topology suitable for renewable energy-based dc bipolar network applications. As given in Figure 1 the CSC converter and Cuk converter produce a negative voltage whereas the SEPIC converter produces a positive voltage at the load output terminal.

≡ SEPIC converter:

The Single-Ended Primary Inductance Converter or SEPIC converter is a modification of a non-isolated DC-DC converter. Some of the features, which makes this converter suitable for the PV application, are given by[14], [15]

- Non-inverted output.
- The input inductor provides a low input ripple and noise.

- Multiple inductors can be a couple in the same core.
- Galvanic isolation can be easily obtained by replacing one of the inductors by a high-frequency transformer.

The conventional SEPIC converter is shown in Figure 3 Where Vg is termed as an input dc voltage source. A MOSFET can be used as switch S, which is having a duty cycle of D.

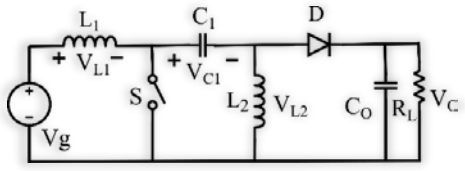

Figure 3. SEPIC Converter topology

In continuous conduction mode, the SEPIC converter operates in two different modes shown in Figure 4a and 4b. In mode (a) when the switch S is turned on (duration is giving by $0 \le t \le DT$, Where T represents the time period of the gate pulse), both the inductor current (I_{L1} and I_{L2}) are increasing because of charging and no energy is transferred to the load as D became reversed biased. In mode (b), when the switch S is turned off (duration given by $DT \le t \le T$), the D becomes forward biased and the energy is transferred to the load as both the inductor (I_{L1} and I_{L2}) are now discharging

The volt-second balance across the inductor L_1 and L_2 given by

$$V_g DT + \left(V_g - V_{C1} - V_D - V_O\right)(1-D)T = 0 \quad (7)$$

$$V_{C1} DT + \left(-V_O - V_D\right)(1-D)T = 0 \quad (8)$$

where V_D represents the voltage drop across the diode.

The output of the SEPIC converter is represented as

$$V_O = \frac{DV_g}{(1-D)} \quad (9)$$

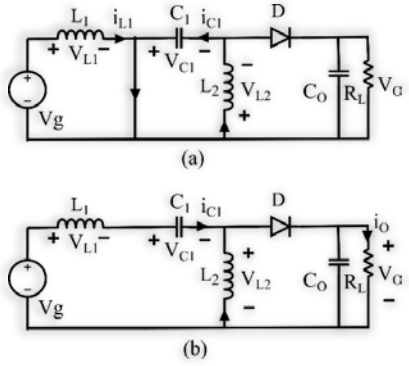

Figure 4. Operation of SEPIC converter. (a) When S is turned on. (b) When S is turned off.

The value L_1, C_1 and L_2 of the SEPIC converter can be calculated by [16]

$$L_1 = \frac{V_g D}{\Delta I_{L1} . f_s} \quad (10)$$

$$L_2 = \frac{V_g D}{\Delta I_{L2} . f_s} \quad (11)$$

$$C_1 = \frac{V_O D}{R_L \Delta V_O f_s} \quad (12)$$

≡ **Cuk Converter:**

Cuk converter is a cascaded combination of the basic boost converter and buck converter with a coupling capacitor. The basic structure of the Cuk converter is given in Figure 5. Energy is transferred from the input side to the output side through the coupling capacitor.

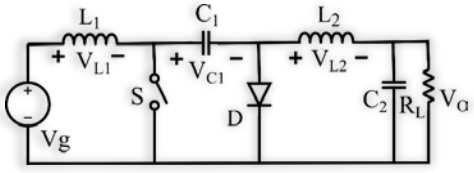

Figure 5. Basic Cuk Converter Circuit

The features of the Cuk converter are:

- Input and output current is continuous in nature.
- Low switching losses and higher efficiency.
- Have low noise generation.
- Low electromagnetic interference and

As it is a combination of buck-boost dc-dc converter, it can able to deliver output voltage both greater and less than the input voltage. The operation of Cuk converter can be divided in two modes (a) and (b) as shown in Figure 6.

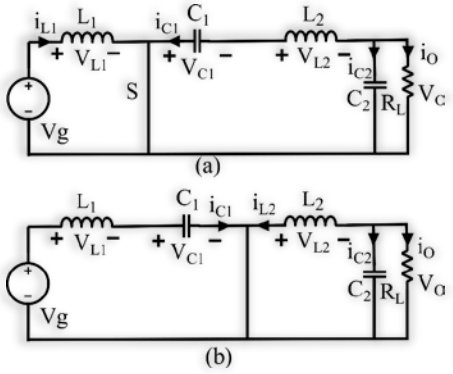

Figure 6. Operation of Cuk Converter, (a) when S is turned on. (b) When S is turned off.

Mode (a) begins when the switch S is turned on (duration is giving by $0 \le t \le DT$). At this mode current through the inductor L_1 increase as it is getting charged by the input voltage. On the other side C_1 is discharging through the output capacitor C_2 and the inductor L_2 by making diode D reverse biased. On the other mode (b) begins when switch S is turned off (duration is giving by $DT \le t \le T$). In this mode diode, D became short-circuited which help the capacitor C_1 to get charged by the supplied voltage, and the inductor L_2 transfer the energy to the load by getting discharged. So, the coupling capacitor C_1 is transferring the energy from source to load by charging and discharging. The load voltage became negative as in both the mode the current flowing through the load is opposite in direction.

Applying volt-second balance across the inductor L_1,

$$V_g DT + \left(V_g - V_{C1}\right)(1-D)T = 0 \quad (13)$$

$$V_{C1} = \frac{V_g}{(1-D)} \quad (14)$$

Applying volt-second balance across the inductor L_2

$$(V_O + V_{C1})DT + V_O(1 - D)T = 0 \quad (15)$$

$$V_O = -\frac{DV_g}{(1 - D)} \quad (16)$$

Equation (16) Represent the output of the Cuk converter. Applying the power balance the value of the current I_{L1} given as

$$I_{L1} = \frac{D^2}{(1 - D)^2}\frac{V_g}{R_L} \quad (17)$$

Voltage ripple across the capacitor C_1 is calculated as

$$\Delta V_{C1} = \frac{D^2 V_g T}{R_L C_1 (1 - D)} \quad (18)$$

≡ Canonical Switch Cell (CSC) Converter:

CSC converter is a modification of a buck-boost converter with having fewer no of devices as shown in Figure 7.

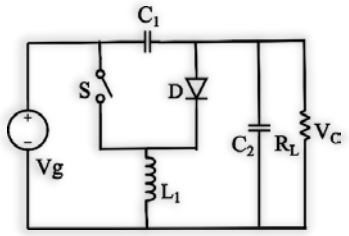

Figure 7. CSC converter circuit

The operation of the converter is divided in two different modes (a) and (b). At mode (a), as the switch S is turned on, the input inductor L_1 is getting charged from the source Vg. Simultaneously the capacitor C_1 discharges its store energy to L_1 through the switch S, as the diode became reversed bias. Mode (b) begins when the switch S became turned off. Then the diode becomes forward biased and then the input inductor L_1 discharges its energy to the output capacitor C_2. Besides that, the capacitor C_1 is also getting charged by the input voltage through diode D, as shown in Figure 8.

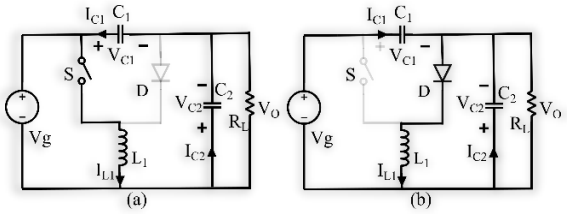

Figure 8. Operation of CSC converter.(a) When S is turned on. (b) When S is turned off.

The expression of the capacitor C_1 and C_2 are calculated as[17]

$$C_1 = \frac{V_g D}{\Delta V_{C1} R_L f_s} \quad (19)$$

$$C_2 = \frac{I_O}{2\omega_L \Delta V_O} \quad (20)$$

where R_L represent the equivalent DC load resistance, ω_L represent the angular frequency of the line voltage.

CONTROL ANALYSIS

As the SIMO converter is feed from the SPV supply, the primary purpose of the controller is to maintain a maximum power extraction from the SPV throughout the operation. Figure 9 shows the block diagram of the proposed converter control system. A feed forward controller consist of a MPPT controller and an Input Voltage Controller (IVC) has considered as total control system. After taking inputs (V_{PV} and I_{PV}) from the SPV panel, the MPPT controller develop a reference voltage V_{PV}^* with the help of PSO algorithm. Then an error signal is generated after comparing the reference signal with the SPV output voltage. There after this error signal is given as a input to the IVC and The signal D_1 is developed. An equivalent 10kHz PWM signal is generated by the PWM generator by taking the D_1 as an input.

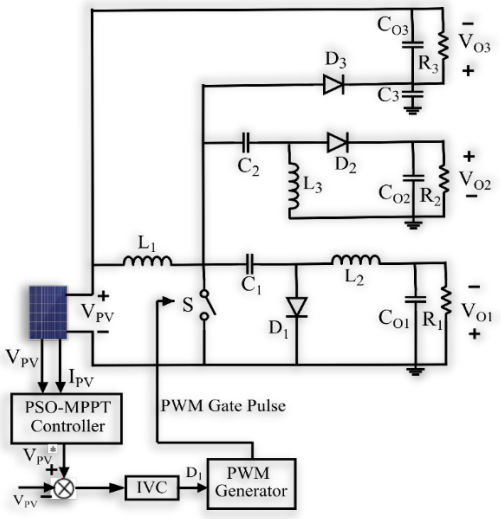

Figure 9. Overall block diagram of total system

The transfer function of the proposed converter is calculated with the help of small signal modelling. After replacing the different component value the transfer function of the proposed converter is given by,

$$TF = \frac{-6.845s^3 - 2.252e^{04}s^2 - 4.33e^{05}s - 1.07e^{06}}{s^3 + 281.6s^2 + 4361s + 1.277e^{04}} \quad (21)$$

To find out the stability of the input loop magnitude and phase plot are plotted which is shown in the figure 10(a). A PID based compensator is designed to improve the stability margin and the improvement of the margins are displayed in the figure 10(b).

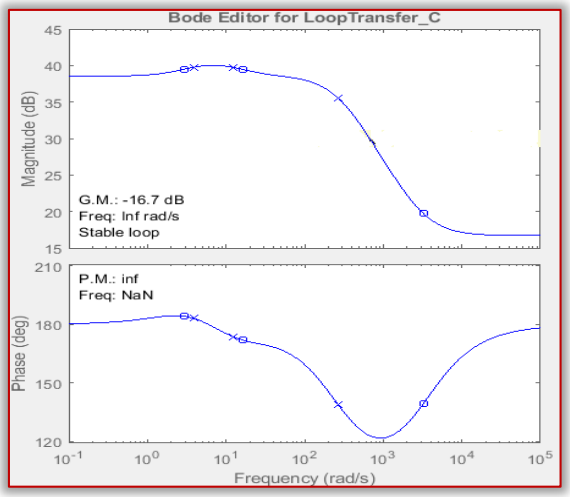

(a)

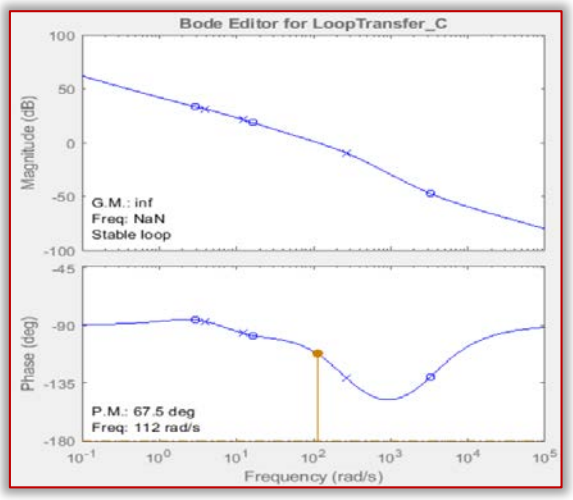

(b)

Figure 10. Magnitude plot and Phase plot of the Transfer function. (a) Without Compensator. (b) With Compensator

SIMULATION RESULTS

In order to verify the PSO-MPPT based SEPIC-Cuk-CSC combinational converter characteristics, a simulation is performed in MATLAB as shown in Figure 11 the details of the SPV panel and the SIMO converter component specification, which is used in this simulation is given in the table-1.

Table -1 Component specification

Name	Rating
Input Panel Power	65W
Open circuit Voltage (Voc)	22V
Voltage at MPP (Vmpp)	18.2V
Short Circuit current (Isc)	5.5A
Current at MPP (Impp)	3.55A
Inductor L1	30mH
Inductor L2 and L3	1.35mH
Capacitor C1	220µF
Capacitor C2	470µF
Resistance R1-R3	80Ω
Switching Frequency	10kHz

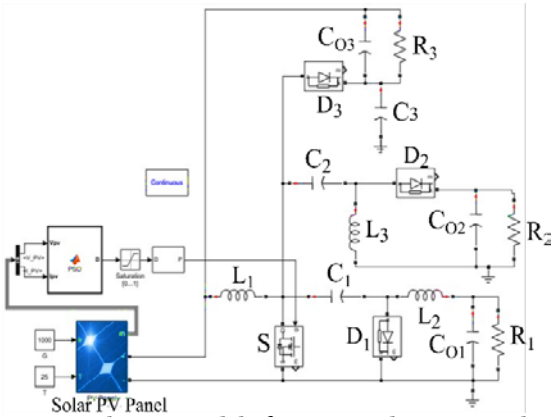

Figure 11. Simulation Model of SEPIC-Cuk-CSC Combination Converter

Fig 12(a) shows the PWM gate pulse of 10 kHz developed by the PSO-MPPT The SPV panel output voltage and the SPV panel extracted power is shown in Fig 12(b) and 12(c) respectively. A swing of SPV voltage around the Vmpp can be observed, which signifies a satisfactory execution of MPPT.

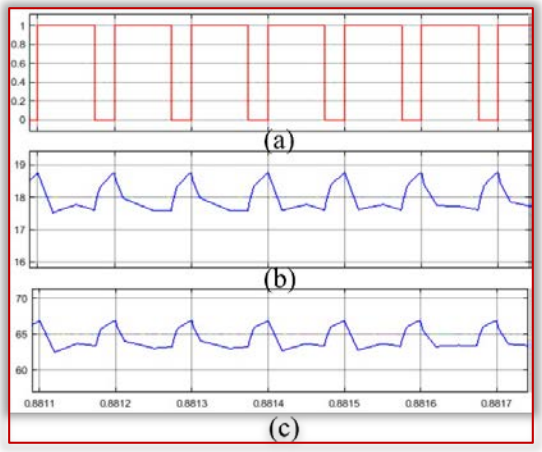

Figure 12. (a) PWM output of the PSO-MPPT controller. (b) SPV panel output voltage (c) Solar PV panel output Power

In Fig 13(b) and Fig 13(d), the charging current of the inductor L_1 and the discharging current of the inductor L_2 are clearly observed during the switch turn-on time. Besides that, the charging and the discharging of the capacitor C_1 is also shown in the Figure 13(c). Similarly, the charging and discharging of the capacitor C_2 along with the inductor L_3 of the SEPIC converter is shown in Figure 14.

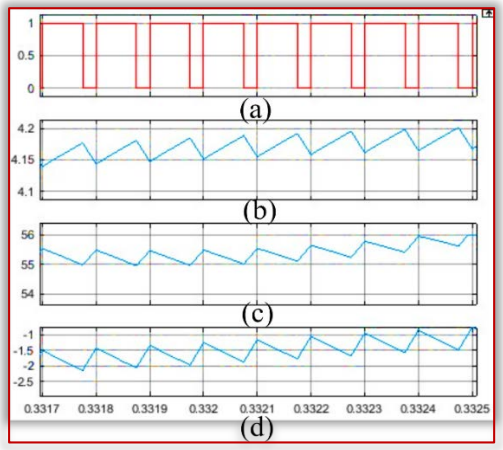

Figure 13. Cuk converter output (a) PWM Gate pulse of switch S. (b) L1 inductor current. (c)The voltage across capacitor C1. (d) L2 inductor current.

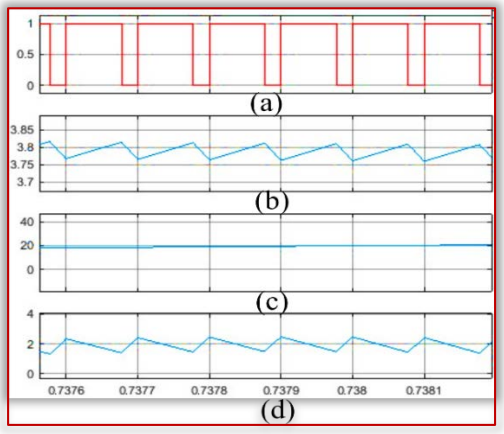

Figure 14. SEPIC converter output (a) PWM Gate pulse of switch S.(b) L1 inductor current. (c)Voltage across capacitor C2. (d) L3 inductor current.

Different characteristics of CSC converter are shown in the Figure 15. Three different voltage output with proper polarity is shown in Fig 16. Where SEPIC and Cuk converter produces almost 48V and -48V. Besides, CSC converter is developing a voltage around -18V. The currents of the three converters is shown in Figure 17. CCM operation is observed in the Cuk and CSC converter.

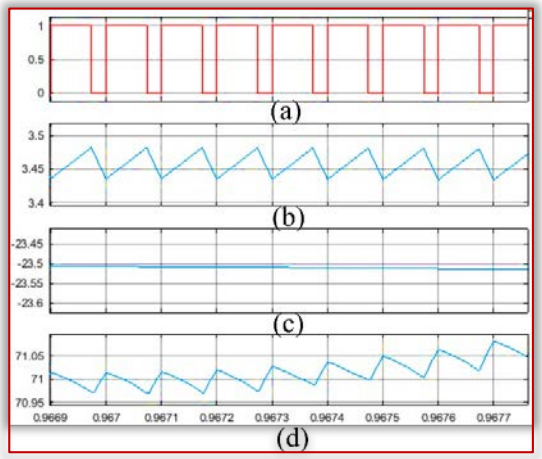

Figure 15. CSC converter output. (a) PWM Gate pulse of switch S. (b) L1 inductor current. (c)The voltage across capacitor C_{O3}. (d) The voltage across capacitor C_3.

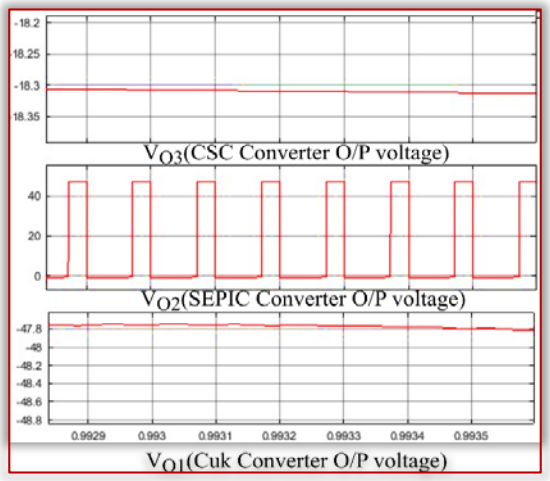

Figure 16. Multiple output voltage of SIMO converter.

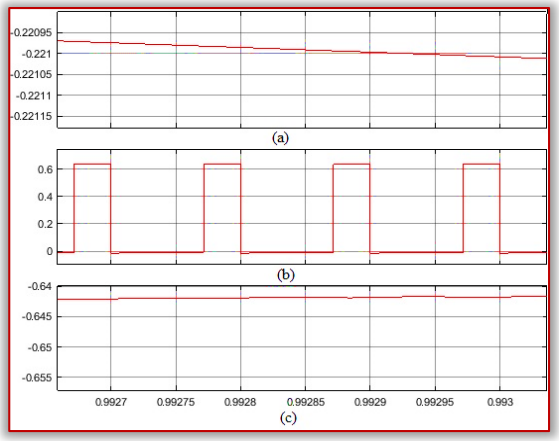

Figure 17. Multiple output current of SIMO converter. (a) CSC converter output current. (b) SEPIC converter output current. (c) Cuk converter output current.

CONCLUSION

This paper presents a design of the SEPIC-Cuk-CSC combination converter used for renewable energy applications. A PSO based MPPT method is applied to extract maximum power. According to the simulation results, it is observed that the PSO method is successfully able to track the MPP in all the conditions. Reduction of design cost and the loss are achieved by reducing the component requirement for developing multiple output voltage levels. As a future scope of this work design of SPWM based inverter can be incorporated with this system as it will helpful to transfer the power to the AC grid.

References

[1] R. J. Wai, W. H. Wang, and C. Y. Lin, "High-performance stand-alone photovoltaic generation system," *IEEE Trans. Ind. Electron.*, vol. 55, no. 1, pp. 240–250, 2008

[2] H. Patel and V. Agarwal, "Maximum power point tracking scheme for PV systems operating under partially shaded conditions," *IEEE Trans. Ind. Electron.*, vol. 55, no. 4, pp. 1689–1698, 2008

[3] M. M. A. Salama, M. Z. Shams El-Dein, and M. Kazerani, "Optimal Photovoltaic Array Recon fi guration to Reduce Partial Shading Losses," *Ieee Trans. Sustain. Energy*, vol. 4, no. 1, pp. 145–153, 2013.

[4] B. Subudhi and R. Pradhan, "A comparative study on maximum power point tracking techniques for photovoltaic power systems," *IEEE Trans. Sustain. Energy*, vol. 4, no. 1, pp. 89–98, 2013

[5] F. D. Murdianto, M. Z. Efendi, R. E. Setiawan, and A. S. L. Hermawan, "Comparison method of MPSO, FPA, and GWO algorithm in MPPT SEPIC converter under dynamic partial shading condition," *Proceeding - ICAMIMIA 2017 Int. Conf. Adv. Mechatronics, Intell. Manuf. Ind. Autom.*, pp. 315–320, 2018

[6] B. K. Panigrahi and P. R. Thakura, "Implementation of Cuk converter with MPPT," *Proc. 3rd IEEE Int. Conf. Adv. Electr. Electron. Information, Commun. Bio-Informatics, AEEICB 2017*, pp. 105–110, 2017

[7] S. Samantara, B. Roy, R. Sharma, S. Choudhury, and B. Jena, "Modeling and simulation of integrated CUK converter for grid connected PV system with EPP MPPT hybridization," *2015 IEEE Power, Commun. Inf. Technol. Conf. PCITC 2015 - Proc.*, pp. 397–402, 2016

[8] J. Chen, D. Maksimović, and R. Erickson, "Buck-boost PWM converters having two independently controlled switches," *PESC Rec. - IEEE Annu. Power Electron. Spec. Conf.*, vol. 2, pp. 736–741, 2001

[9] B. Lin, S. Member, and F. Hsieh, "Soft-Switching Zeta – Flyback Converter With a Buck – Boost Type of Active Clamp," vol. 54, no. 5, pp. 2813–2822, 2007.

[10] M. B. Ferrera, S. P. Litran, E. Duran, and J. M. Andujar, "A SEPIC-Cuk converter combination for bipolar DC microgrid applications," *Proc. IEEE Int. Conf. Ind. Technol.*, vol. 2015-June, no. June, pp. 884–889, 2015

[11] H. Renaudineau *et al.*, "A PSO-based global MPPT technique for distributed PV power generation," *IEEE Trans. Ind. Electron.*, vol. 62, no. 2, pp. 1047–1058, 2015

[12] K. Ishaque, Z. Salam, M. Amjad, and S. Mekhilef, "An improved particle swarm optimization (PSO)-based MPPT for PV with reduced steady-state oscillation," *IEEE Trans. Power Electron.*, vol. 27, no. 8, pp. 3627–3638, 2012

[13] M. A. Abdullah, T. Al-Hadhrami, C. W. Tan, and A. H. Yatim, "Towards green energy for smart cities: Particle swarm optimization based MPPT approach," *IEEE Access*, vol. 6, pp. 58427–58438, 2018
[14] E. Durán, J. Galán, J. M. Andújar, D. D. I. Electrónica, D. S. Infor, and U. De Huelva, "A N ew A pplication of the B uck - B oost -D erived C onverters to O btain the I-V C urve of P hotovoltaic M odules," pp. 413–417, 2007.
[15] J. J. Chacon, R. A. Ortiz, J. E. Archila, M. A. Mantilla, M. A. Botero, and J. F. Petit, "Prototype for the characterization of photovoltaic panels based on a SEPIC converter," pp. 1–6, 2017
[16] M. O. Ali and A. H. Ahmad, "Design, modelling and simulation of controlled sepic dc-dc converter-based genetic algorithm," *Int. J. Power Electron. Drive Syst.*, vol. 11, no. 4, pp. 2116–2125, 2020
[17] V. Bist and B. Singh, "A PFC-Based BLDC motor drive using a canonical switching cell converter," *IEEE Trans. Ind. Informatics*, vol. 10, no. 2, pp. 1207–1215, 2014

ISSN: 2067-3809